Stark-ladder resonances in piezoelectric composites

G. Monsivais,[1,*] R. Rodríguez-Ramos,[2,3] R. Esquivel-Sirvent,[1] and L. Fernández-Alvarez[4]
[1]*Instituto de Física, Universidad Nacional Autónoma de México, Apartado Postal 20-364, Distrito Federal 01000, México*
[2]*Facultad de Matemáticas y Computación, Universidad de la Habana, San Lazaro y L. Velado, 10400, Habana 4, Cuba*
[3]*Instituto de Ingeniería, Universidad Nacional Autónoma de México, Apartado Postal 70-472, Distrito Federal 01000, Mexico*
[4]*AMS, Parque Empresarial de la Moraleja, Avenida de Europa 24, Alcobendas 28108, Spain*
(Received 1 February 2002; revised manuscript received 19 February 2003; published 26 November 2003)

In this paper we introduce a piezoelectric composite medium. The composite shows a series of resonances similar to the Stark-ladder resonances originally observed in the propagation of electrons through crystals in a dc electric field. These resonances appear when shear horizontal and surface waves propagate through a special piezoelectric composite medium consisting of N piezoelectric layers, each layer being a material of hexagonal $6mm$ symmetry. For periodic piezocomposites, we obtain a band structure as expected. However, when the periodicity is broken by adding a linear term in the values of the piezoelectric parameters of the layers, the band structure is destroyed and, in certain cases, resonances of Stark-ladder type appear instead. A 4×4 transfer matrix approach is used to calculate the response of the composite under electromechanical perturbations. The response is studied as a function of the properties of the different materials, width of the layers, wave frequency, and angle of incidence. Numerical results for the electric potential and for the displacement of the surface of the last layer of the composite are presented showing the existence of Stark-ladder resonances.

DOI: 10.1103/PhysRevB.68.174109 PACS number(s): 77.65.Fs, 77.65.Dq, 77.90.+k

I. INTRODUCTION

The study of new materials is one of the most active fields of science and technology; in particular, piezoelectric materials have a special place and have gained considerable attention. On the one hand, there are many applications, such as ultrasonic transducers, hydrophone technologies, etc., in which they play an important role. On the other hand, new piezocomposites appear frequently with novel properties and applications, which require an appropriate theoretical description. The most common arrangement of piezoelectric material for transducer applications has been layered systems such as the original steel-quartz sandwich conceived by Langevin.[1] The layered configurations are easy to obtain experimentally and their response can be modified by a suitable choice of materials.[2] Recently, such types of configurations have been investigated by many authors.[3–5] In particular, the theory of propagation of waves through periodic systems is well established and the band structure in the dispersion-relation characteristics for these systems has been measured and calculated in the quantum, photonic, elastic, and piezoelectric cases. However, when the periodicity is broken interesting effects arise, such as Anderson localization.

The purpose of this paper is to introduce a layered piezocomposite whose transport properties show another interesting effect consisting of a series of resonances similar to the Stark ladders (SL's) first studied by Wannier[6] in connection with the energy spectrum of an electron traveling through a crystal in a dc electric field. This system could be used as a very selective filter. The new piezocomposite is studied using a theoretical model and some of its properties are numerically calculated. The calculations become more difficult because the piezoelectric materials combine both the electromagnetic and the elastic case.

The SL studied by Wannier are a series of electronic states whose associated energies $E_1, E_2, \ldots, E_n, \ldots$ are equally spaced; the separation between adjacent energies $E_i - E_{i-1}$ is proportional to the electric field strength. In order to introduce our notation and for future reference we reproduce briefly Wannier's arguments supporting the existence of the SL. Let us analyze the properties of Schrödinger's equation for an electron of mass m_e and charge e in the presence of a potential $\mathcal{V}(x)$. This potential is due to an electric field of strength $\mathcal{E}$ plus a periodic potential $V_p(x)$ of period p. Thus, $\mathcal{V}(x) = -\mathcal{E}x + V_p(x)$ and Schrödinger's equation reads

$$-\frac{\hbar^2}{2m_e}\frac{d^2\Psi(x)}{dx^2} + e\mathcal{V}(x)\Psi(x) = E\Psi(x), \tag{1}$$

where $\Psi(x)$ is the wave function and E is the electronic energy (the $\mathcal{E}=0$ case corresponds to a periodic potential and the electronic spectrum shows the well-known band structure). Let us make the change of variable $x' = x - mp$, m being an arbitrary integer. Since $\mathcal{V}(x)$ has the crucial property

$$\mathcal{V}(x'+mp) = \mathcal{V}(x') - mp\mathcal{E}, \quad \forall x' \in R, \tag{2}$$

we obtain

$$-\frac{\hbar^2}{2m_e}\frac{d^2\Psi(x'+mp)}{dx^2} + e[\mathcal{V}(x') - mp\mathcal{E}]\Psi(x'+mp) = E\Psi(x'+mp). \tag{3}$$

Defining $\Phi(x) = \Psi(x'+mp)$ we get an equation similar to Eq. (1) but with the energy $E + mpe\mathcal{E}$, i.e.,

$$-\frac{\hbar^2}{2m_e}\frac{d^2\Phi(x)}{dx^2} + e\mathcal{V}(x)\Phi(x) = (E + mpe\mathcal{E})\Phi(x). \tag{4}$$

By comparing Eqs. (1) and (4) we conclude that if there exists a solution $\Psi(x)$ associated with the energy E there must exist a solution $\Phi(x)$ associated with the energy $E+mpe\mathcal{E}$. Since m is an arbitrary integer, we obtain a series of solutions whose energies are separated by a distance $pe\mathcal{E}$, i.e., one Stark ladder. We observe, however, that the spectrum for this system is continuous and therefore a family of such solutions could be indistinguishable from the continuum and the concept of SL would make no sense. However, when the system has states with special characteristics, such as resonant states, they become distinguishable from the continuum. These are the Stark-ladder resonances (SLR). Thus, we see that the electric field has a qualitatively dramatic effect on the electronic spectrum.

It is interesting to mention that for many years[7–11] the existence of the SLR in the electronic spectrum was controversial until they were finally experimentally observed.[12] We should mention that they were first observed in numerical calculations of unidimensional simplified models.[13–17] In these cases, since the numerical models are of finite extent, Eq. (2) is not satisfied exactly and the SLR are not perfect. The same is true for real systems.

The SLR are analogous to the Landau levels which appear in a system of electrons in a magnetic field. Both phenomena (the SLR in the electronic spectrum and the Landau levels) belong to the field of quantum physics. The resonances we will study here belong to the field of classical physics. As we will see, they are resonances in the elastic properties of some piezocomposites.

In this paper we study layered piezocomposites with a free surface at one end of the system with piezoelectric waves impinging on the other side. The response of the system is described by the displacement of the free surface and by the electric potential. As in the quantum-mechanical case, there could be other nonequivalent configurations which could also show a structure of SLR and these could be described in other forms.[18] However, this paper is only devoted to systems with the configuration mentioned above. In Secs. III and IV the method of solution and the appropriate boundary conditions are discussed. Finally, the results and conclusions are presented in Secs. V and VI, respectively.

II. THE MODEL

Let us consider the piezoelectric composite shown in Fig. 1. It is embedded within two semi-infinite media; the one located to the left is a piezoelectric and the other one is vacuum. The system is composed of N piezoelectric homogeneous layers with $6mm$ symmetry. The OY axis was chosen perpendicular to the interfaces. We define layer n as the layer between the boundaries located at y_n and y_{n+1}. The layer associated with the value $n=-1$ is the left semi-infinite substrate and the one associated with the value $n=N-1$ is the last piezoelectric layer at the right end of the composite. Thus $-1\leqslant n\leqslant N-1$.

The thickness of even (odd) layers is equal to p_1 (p_2). The nth layer is characterized by its macroscopic properties by means of the following tensor quantities: the tensor of elastic moduli $c_{ij}^{(n)}$, the tensor of piezoelectric moduli $e_{ij}^{(n)}$,

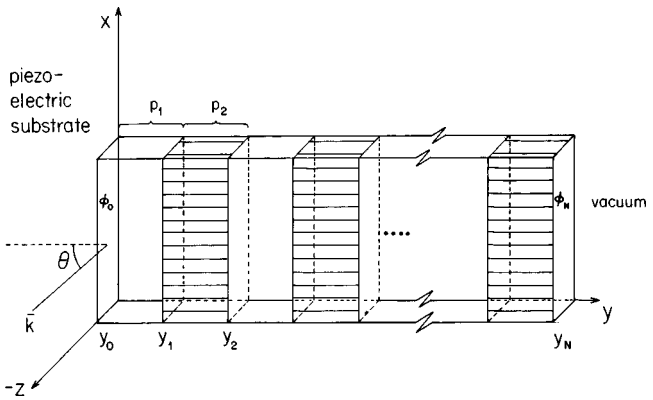

FIG. 1. The piezocomposite is a layered structure whose interfaces are perpendicular to the OY axis and located at points y_0, $y_1,\ldots,y_N$. The widths p_1 and p_2 are defined as y_1-y_0 and y_2-y_1, respectively. The width of the layers is periodic with period $p=p_1+p_2$. To the left of the system we have a piezoelectric substrate where a piezoelectric SH wave impinges on the system with *wave vector* **k**. The substrate is taken as the layer number -1.

the dielectric permittivity tensor $\epsilon_{ij}^{(n)}$, and the mass density $\rho^{(n)}$ (see Fig. 2). The values of these quantities obey a very particular relation as will be discussed in Sec. III in connection with Eq. (17). We want to analyze the propagation of a shear horizontal (SH) piezoelectric wave with *wave vector* **k** that impinges at an angle θ from a left semi-infinite substrate upon the layered heterogeneous piezoelectric medium. Let us assume that the wave propagates in the XY plane, and it is polarized along the OZ axis. The system and scattering process are sketched in Figs. 1 and 2.

III. SOLUTION TO THE PROBLEM

The system described above can be studied using the continuum mechanics approach, in particular the dynamic equations of elasticity and Gauss equation for electromagnetism, using the quasistatic approximation for the electric potential.

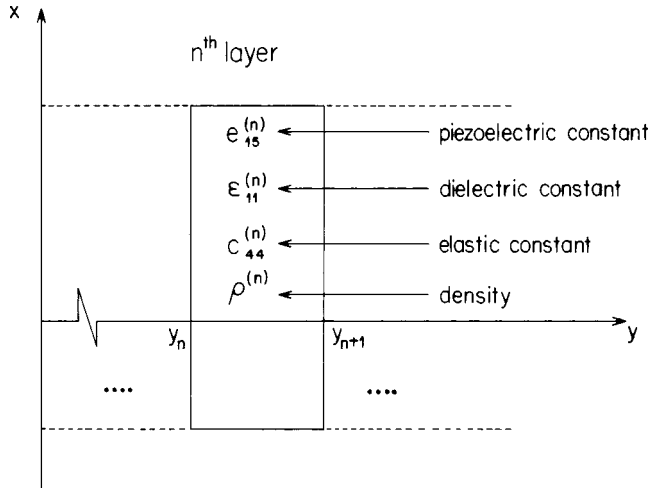

FIG. 2. The (nth) layer of the system is a homogeneous material of hexagonal $6mm$ symmetry characterized by the parameters $e_{15}^{(n)}$, $\epsilon_{11}^{(n)}$, $c_{44}^{(n)}$, and $\rho^{(n)}$ as defined in the figure.

Since the composite consists of a set of homogeneous layers we will use the equations of piezoelectricity for each layer (see Appendix A) and then we will match the different solutions at the boundary of the layers.

It can be shown that the equations of piezoelectricity admit solutions where the shear vertical and SH waves are separated. The SH waves correspond to the nontrivial solution of the system of Eqs. (A7)–(A10) of Appendix A with $u_1=u_2=0$, $u_3\neq 0$, and $\phi\neq 0$, u_i being the components of the displacement vector $\vec{u}=(u_1,u_2,u_3)$. Under the last considerations the system involves the u_3 and the electric potential ϕ as follows [for simplicity, we will omit the superscript (n) in these basic equations]:

$$c_{44}\left(\frac{\partial^2 u_3}{\partial x^2}+\frac{\partial^2 u_3}{\partial y^2}\right)+e_{15}\left(\frac{\partial^2 \phi}{\partial x^2}+\frac{\partial^2 \phi}{\partial y^2}\right)=\rho\ddot{u_3}, \tag{5}$$

$$e_{15}\left(\frac{\partial^2 u_3}{\partial x^2}+\frac{\partial^2 u_3}{\partial y^2}\right)-\epsilon_{11}\left(\frac{\partial^2 \phi}{\partial x^2}+\frac{\partial^2 \phi}{\partial y^2}\right)=0. \tag{6}$$

Since the piezocomposite is homogeneous in the OX and OZ directions we can consider only solutions of Eqs. (5) and (6) of the form

$$u_3(x,y,t)=\tilde{u}_3(y)e^{i(k_x x-\omega t)}, \tag{7}$$

$$\phi(x,y,t)=\tilde{\phi}(y)e^{i(k_x x-\omega t)}, \tag{8}$$

where $\tilde{u}_3(y)$ and $\tilde{\phi}(y)$ satisfy the matrix equation

$$\begin{pmatrix}\frac{d^2\tilde{u}_3}{dy^2}\\ \frac{d^2\tilde{\phi}}{dy^2}\end{pmatrix}+\frac{\rho\omega^2}{\bar{c}_{44}}\begin{pmatrix}1 & 0\\ \frac{e_{15}}{\epsilon_{11}} & 0\end{pmatrix}\begin{pmatrix}\tilde{u}_3\\ 0\end{pmatrix}=k_x^2\begin{pmatrix}\tilde{u}_3\\ \tilde{\phi}\end{pmatrix}, \tag{9}$$

with $\bar{c}_{44}\equiv c_{44}+(e_{15}^2/\epsilon_{11})$. The above equation is satisfied in each layer but with different values of the parameters ρ, e_{15}, c_{44}, and ϵ_{11} from layer to layer. However, k_x is the same in all layers due to the Snell law. Therefore the equation governing the whole system can be written as

$$\frac{d^2}{dy^2}\begin{pmatrix}\tilde{u}_3\\ \tilde{\phi}\end{pmatrix}+\frac{\rho(y)\omega^2}{\bar{c}_{44}(y)}\begin{pmatrix}1 & 0\\ \frac{e_{15}(y)}{\epsilon_{11}(y)} & 0\end{pmatrix}\begin{pmatrix}\tilde{u}_3\\ \tilde{\phi}\end{pmatrix}=k_x^2\begin{pmatrix}\tilde{u}_3\\ \tilde{\phi}\end{pmatrix}, \tag{10}$$

where $\rho(y)=\rho^{(n)}$ for $y_n<y<y_{n+1}$ and similar relations for the other parameters. The quantity $k(y)\equiv[\rho(y)\omega^2/\bar{c}_{44}(y)]^{1/2}$ is the *wave number* at the $(n$th) layer for $y_n<y<y_{n+1}$. Thus, the magnitude of the incident *wave vector* **k** of Fig. 1 is equal to $k(-1)$. Furthermore, $k_x=k(-1)\sin\theta$. In general, due to the column of zeros in the matrix of the second term, this equation cannot be handled as it was done with Eq. (1) in order to obtain Eq. (4). Therefore, we cannot conclude from Eq. (10) that the system must have resonances of the SL type. However, the electric potential in each layer is a linear combination of two parts:[19] one of them is proportional to the mechanical displacements and the other is equal to a sum of two surface waves located at the ends of each layer, i.e.,

$$\tilde{\phi}(y)=\tilde{\phi}_1(y)+\tilde{\phi}_2(y), \tag{11}$$

with

$$\tilde{\phi}_1(y)=\frac{e_{15}(y)}{\epsilon_{11}(y)}\tilde{u}_3(y)=\frac{e_{15}(y)}{\epsilon_{11}(y)}(Ae^{ik_y(y)y}+Be^{-ik_y(y)y}), \tag{12}$$

$$\tilde{\phi}_2(y)=\frac{e_{15}(y)}{\epsilon_{11}(y)}(Ce^{k_x(y-y_n)}+De^{-k_x(y-y_n)}), \tag{13}$$

and

$$k_y^2(y)=\frac{\rho(y)\omega^2}{\bar{c}_{44}(y)}-k_x^2=k^2(y)-k_x^2. \tag{14}$$

Then Eq. (10) becomes

$$\frac{d^2}{dy^2}\begin{pmatrix}\tilde{u}_3\\ \frac{e_{15}(y)}{\epsilon_{11}(y)}\tilde{u}_3\end{pmatrix}+\frac{d^2}{dy^2}\begin{pmatrix}0\\ \tilde{\phi}_2\end{pmatrix}+\frac{\rho(y)\omega^2}{\bar{c}_{44}(y)}\begin{pmatrix}\tilde{u}_3\\ \frac{e_{15}(y)}{\epsilon_{11}(y)}\tilde{u}_3\end{pmatrix}=k_x^2\begin{pmatrix}\tilde{u}_3\\ \frac{e_{15}(y)}{\epsilon_{11}(y)}\tilde{u}_3\end{pmatrix}+k_x^2\begin{pmatrix}0\\ \tilde{\phi}_2\end{pmatrix}. \tag{15}$$

Since $d^2\tilde{\phi}_2/dy^2=k_x^2\tilde{\phi}_2$, Eq. (15) is then converted into a unique ordinary differential equation valid within the layers (the matching properties at the interphases will be analyzed in Sec. IV):

$$\frac{d^2\tilde{u}_3}{dy^2}+\frac{\rho(y)\omega^2}{\bar{c}_{44}(y)}\tilde{u}_3=k_x^2\tilde{u}_3. \tag{16}$$

Now the structure of Eq. (16) is already similar to Schrödinger equation (1) used by Wannier[6] to predict the existence of RSL in the energy spectrum of an electron. Therefore, if a piezoelectric multilayer is constructed in such a way that $\rho(y)\omega^2/\bar{c}_{44}(y)$ satisfied a relation of the form as Eq. (2), Ref. 20, one could suspect the existence of similar resonances in our system although not in the energy spectrum but in the values of k_x^2. In order to see this clearly, before continuing with the solution of the problem, it is convenient to reproduce Wannier's arguments adapted to our piezocomposites.

We recall that the piezocomposite consists in a series of pairs of layers whose widths are p_1 and p_2, respectively. Furthermore, the width of the layers is periodic with period $p=p_1+p_2$ (see Figs. 1 and 2). Now let us suppose that the values of the material parameters obey a linear relation of the form [analogous to Eq. (2)]

$$\left(\frac{\rho\omega^2}{\bar{c}_{44}}\right)^{(n+2m)}=\left(\frac{\rho\omega^2}{\bar{c}_{44}}\right)^{(n)}+mpF,\quad \forall n,m\in N, \tag{17}$$

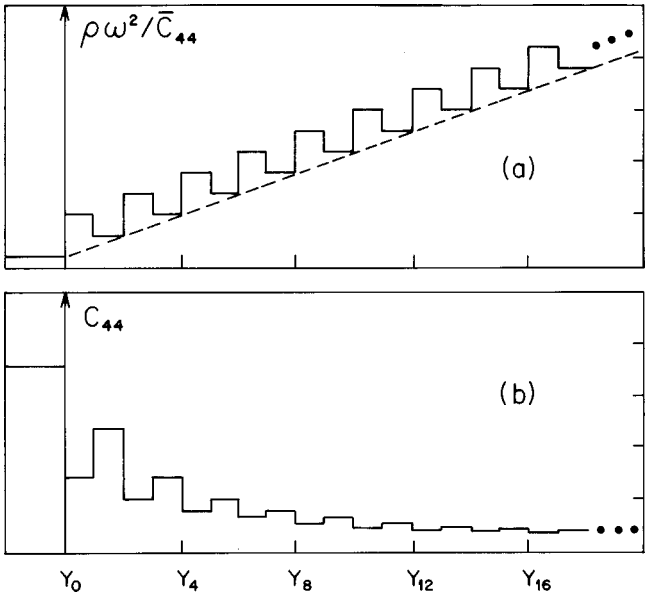

FIG. 3. (a) Plot of $\rho(y)\omega^2/\overline{c_{44}}(y)$ and (b) plot of c_{44} which satisfy Eqs. (17) and (28), respectively. The slope of the dashed line in (a) is equal to F. When $F=0$ the plots become periodic functions with period p. We use arbitrary units in both figures.

which is represented graphically in Fig. 3(a). Here $(\rho\omega^2/\overline{c_{44}})^{(j)}$represents the values of the magnitude $\rho(y)\omega^2/\overline{c_{44}}(y)$ at the layer j, F an arbitrary constant, and m an arbitrary integer. The particular case $F=0$ corresponds to a periodic system.

Equation (16) applied to the (nth) layer can be written as

$$\frac{d^2\tilde{u}_3}{dy^2}+\left(\frac{\rho\omega^2}{\overline{c_{44}}}\right)^{(n)}\tilde{u}_3=k_x^2\tilde{u}_3. \tag{18}$$

Using the change of variable $y\rightarrow y+mp$ [which in term of the layers means $n\rightarrow n+2m$, see Fig. 3(a)] Eq. (18) becomes

$$\frac{d^2\tilde{u}_3(y+mp)}{dy^2}+\left(\frac{\rho\omega^2}{\overline{c_{44}}}\right)^{(n+2m)}\tilde{u}_3(y+mp)=k_x^2\tilde{u}_3(y+mp). \tag{19}$$

Defining

$$v(y)=\tilde{u}_3(y+mp) \tag{20}$$

and using Eqs. (17), (19), and (20) we obtain

$$\frac{d^2v(y)}{dy^2}+\left(\frac{\rho\omega^2}{\overline{c_{44}}}\right)^{(n)}v(y)=(k_x^2-mpF)v(y). \tag{21}$$

From Eqs. (18) and (21) we conclude that if there exists a solution $\tilde{u}_3(y)$ for Eq. (18) for a given value of k_x^2 then there exists a solution $v(y)$ of Eq. (21) associated to the value (k_x^2-mpF). Therefore, we expect that in a plot $u_3(y)$ vs k_x^2 the structure of the curve will repeat periodically with period pF, i.e., we expect a Stark ladder. Indeed, in order to use normalized quantities we will sketch $u_3(y)$ as a function of $\sin^2\theta$ instead of k_x^2 and the structure of the curve will repeat with period $\Delta S\equiv pF/k^2(-1)=pF\overline{c_{44}}(-1)/[\rho(-1)\omega^2]$.

Similar arguments have been used in order to predict the existence of SLR in elastic and electromagnetic systems.[26–30] However, we must mention that this formulation is not a formal proof for the existence of the SLR; it is only an indication that the SLR could exist. As a matter of fact, these arguments have the same weak points as the ones pointed out by Zak[7] in connection with predictions of Wannier[6] for the SLR in quantum systems. For example, since there are no restrictions in the values of k_x in the interval $[0,k]$, there is no reason to conclude that the only possible values of k_x^2 are $(k_o)_x^2-mpF$ for a fixed k_o. Furthermore, any numerical model or any possible experimental setup has finite length, and it is well known that for such systems the boundary conditions may change the eigenvalues and eigenfunctions giving rise to instabilities in the spectrum for quantum systems.

For the piezoelectric case things are worse. In fact, a more detailed analysis shows that any function of the form $A_ne^{ik_y^n y}+B_ne^{-ik_y^n y}$ for $y\in[y_n,y_{n+1}]$ with arbitrary sets of coefficients $\{A_n\}$, $\{B_n\}$, is a solution to Eq. (18) associated to k_x^2. However, only the function satisfying also the boundary conditions given by Eqs. (29)–(35) is the correct solution to the problem. If we denote $f_{k_x^2}(y)$ and $f_{k_x^2-mpF}(y)$ as the correct solutions associated to k_x^2 and k_x^2-mpF, respectively, it is not necessarily true that $f_{k_x^2}(y+mp)=f_{k_x^2-mpF}(y)$. This is so because the boundary conditions establish relations among the sets of coefficients $\{A_n\}$, $\{B_n\}$ and the sets $\{C_n\}$, $\{D_n\}$ associated to the function $\tilde{\phi}_2(y)$ which does not satisfy an equation of the form of Eq. (16). So we do not know in advance if the interference pattern associated to the waves described by $f_{k_x^2-mpF}(y)$ in the interval $[y_o,y_N]$ is of the same pattern as the one for $f_{k_x^2}(y+mp)$. For example, if the pattern associated with $f_{k_x^2-mpF}(y)$ is a resonance, the pattern associated with $f_{k_x^2}(y+mp)$ could not be one. Therefore, it is necessary to solve the equations explicitly and to analyze the solutions. Our numerical calculations will show that, in spite of the above weak points in the theoretical arguments, the piezoelectric SLR indeed exist, although, as expected, they are more unstable than in other cases.[13,16,17,26,30]

In order to solve the equations, we continue now with the general discussion. Equation (17) can be satisfied in different ways. In this work, for simplicity in further algebra, only the following case is considered as an example: let us assume the material constants (density, elastic, piezoelectric, and dielectric) obey the following rules:

$$e_{15}^{(n)}=c_{44}^{(n)}\Omega, \quad \forall n, \tag{22}$$

$$\epsilon_{11}^{(n)}=e_{15}^{(n)}/\Gamma, \quad \forall n, \tag{23}$$

$$\rho^{(n+m)}=\rho^{(n)}, \quad \forall n,m, \tag{24}$$

which imply

$$\left(\frac{\epsilon_{11}}{c_{44}}\right)^{(n)}=\frac{\Omega}{\Gamma}, \tag{25}$$

$$\overline{c}_{44}^{(n)}\equiv c_{44}^{(n)}(1+\Omega\Gamma), \tag{26}$$

and

$$\Delta S=p\frac{F(1+\Omega\Gamma)}{\rho^{(-1)}\omega^2}c_{44}^{(-1)}=p\,\mathfrak{I}c_{44}^{(-1)}, \tag{27}$$

where Γ, Ω are two constants independent of the index (n) and $\mathfrak{I}\equiv F(1+\Omega\Gamma)/\rho^{(-1)}\omega^2$. Therefore, from Eqs. (17), (22)–(26),

$$\left(\frac{1}{c_{44}}\right)^{(2m+n)}=\left(\frac{1}{c_{44}}\right)^{(n)}+mp\mathfrak{I}. \tag{28}$$

The characteristic form of a function $c_{44}(y)$ satisfying Eq. (28) is shown in Fig. 3(b). The form of $1/c_{44}(y)$ is, of course, similar to the one of $1/\overline{c}_{44}(y)$ [see Fig. 3(a)] but with a slope equal to $\mathfrak{I}$.

IV. BOUNDARY CONDITIONS

. The boundary conditions used can be summarized into two groups: (a) the conditions acting between layers and (b) those acting at the edge of the composite. For the first ones, we consider the continuity of displacement u_3, stress tensor T_{23}, electric displacement D_2, and the electric potential ϕ at the interfaces of the piezocomposite. These conditions can be written in the following form:

$$u_3^{(n)}(y_n)=u_3^{(n-1)}(y_n), \tag{29}$$

$$T_{23}^{(n)}(y_n)=T_{23}^{(n-1)}(y_n), \tag{30}$$

$$D_2^{(n)}(y_n)=D_2^{(n-1)}(y_n), \tag{31}$$

$$\phi^{(n)}(y_n)=\phi^{(n-1)}(y_n), \quad \text{with} \quad 0\leqslant n\leqslant N-1. \tag{32}$$

The boundary conditions at the edges of the composite ($y=y_0$ and $y=y_N$) are the free mechanical action at the boundary $y=y_N$ (right end of the composite) and electric potential ϕ equal to zero at the ends of the composite:

$$T_{23}^{(N-1)}(y_N)=0, \tag{33}$$

$$\phi^{(-1)}(y_0)=0, \tag{34}$$

$$\phi^{(N-1)}(y_N)=0. \tag{35}$$

The other condition comes from the normalization of the incident wave, i.e., the value of A_{-1}.

Using the boundary conditions (29)–(32) we obtain the total transfer matrix M of order (4×4), which relates the coefficients A_{-1}, B_{-1}, C_{-1}, D_{-1} of the left semi-infinite medium $(n=-1)$ with the coefficients A_{N-1}, B_{N-1}, C_{N-1}, D_{N-1} of the last piezoelectric layer $(n=N-1)$ (see Appendix B). The matrix M gives four relations between these coefficients and with the help of Eqs. (33)–(35) we derive three other conditions. Therefore, we have eight conditions (including the normalization condition) in order to determine the same number of unknown coefficients: A_{-1}, B_{-1}, C_{-1}, D_{-1}, A_{N-1}, B_{N-1}, C_{N-1}, D_{N-1}. In the following section we will analyze the numerical solution to these equations.

TABLE I. Parameters used in the calculations. The values of $c_{44}^{(n)}$ for $n=1,2,\ldots$ are obtained from Eq. (28).

Periodic	Nonperiodic
$\mathfrak{I}=0$	$\mathfrak{I}=1/4\times10^{-7}\frac{m}{N}$
$c_{44}^{(-1)}=4/11\times10^{10}\frac{N}{m^2}$	$c_{44}^{(-1)}=4\times10^{10}\frac{N}{m^2}$
$c_{44}^{(0)}=1/4\times10^{10}\frac{N}{m^2}$	$c_{44}^{(0)}=(121/80)^{-1}\times10^{10}\frac{N}{m^2}$

V. RESULTS

There are different ways to define a resonance,[17] not all giving exactly the same quantitative results. One of these definitions is given in terms of the maximum response of the system under the action of external perturbations. Here we used this definition. We have calculated the displacement amplitude $|\tilde{u}_3(y)|$ at the free surface $(y=y_N)$ when an electromechanical wave travels from the substrate to the piezocomposite of Fig. 1. This quantity was calculated as a function of $\sin^2\theta$. The values for the parameters used in the calculations are $N=99$, $p_1=5.0\times10^{-5}$ m, $p_2=15.0\times10^{-5}$ m, $\rho^{(-1)}=2500$ kg/m^3, $\epsilon_{11}^{(-1)}=64.63\times10^{-10}$ F/m, $\Phi_0=0$ V, and $\Phi_N=0$ V. Furthermore, $\mathfrak{I}$ and $c_{44}^{(n)}$ are given in Table I. In this way the structure is 0.985 cm long. The values of the other variables are indicated in each figure.

To understand the response of the laminated system, we analyze the periodic case first [$F=0$ in Eq. (17), or $\mathfrak{I}=0$ in Eq. (28)]. This is depicted in Fig. 4 where we show the

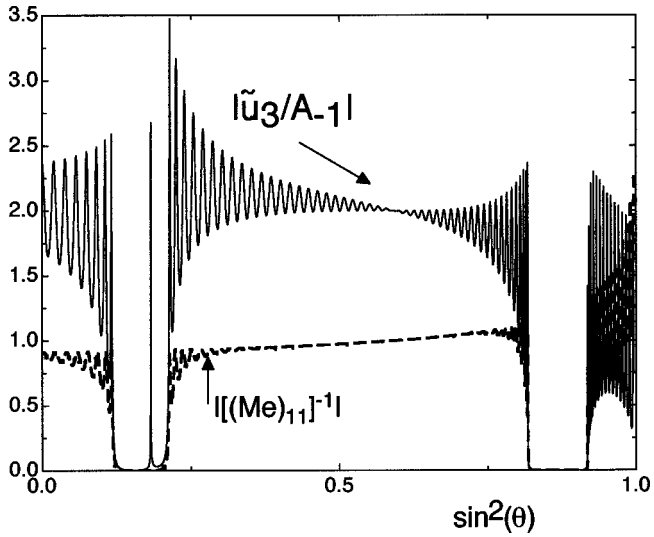

FIG. 4. The solid line (dashed line) is the plot of $|\tilde{u}_3(y_N)/A_{-1}|$ ($|(M_e)_{11}|^{-1}$) as a function of $\sin^2\theta$ for the piezocomposite of Fig. 1 for the periodic case ($F=0$). Both plots show the band structure. The parameters are $\omega=4\times10^7$ s^{-1}, and $e_{15}^{(-1)}=1$ C/m^2.

values of the displacement amplification $|\tilde{u}_3(y_N)/A_{-1}|$ (solid line). From Eq. (12) we observe that $\tilde{u}_3(y_N)/A_{-1}$ is a dimensionless quantity. It is almost equal to zero in some regions and it is near 2 in the remainder, i.e., it has a band structure as it should. The curve shows a central complete band and two incomplete bands as well. The number and width of the bands can be modified by changing the values of the parameters.

It is well known that for the case of homogeneous elastic half space the amplitude of the displacement must be doubled due to the presence of the free surface. The curve shows that for the analyzed piezocomposite $|\tilde{u}_3(y_N)/A_{-1}|$, is, in fact, close to 2 in the bands. Since $0 \leqslant \sin^2\theta \leqslant 1$ the structure of bands exists only in the interval [0,1]. This is an important difference with respect to the quantum case where the role of $k_x^2 = k^2(-1)\sin^2\theta$ is played by E [compare Eqs. (1) and (14)] which can take any real value for an infinite system in a dc electric field.

A more detailed analysis of this curve shows that the number of maxima (resonances) in the complete band is equal to 49. This is so because the curve corresponds to the case $N=99$ (49 complete periods) and therefore the number of complete cells able to catch resonant states is 49. We see also that the curve inside the gap has a resonance near $\sin^2\theta=0.18$ which is not a part of the central band. Indeed, this resonance is associated with a surface state due to the fact that the system has a free surface.

In order to verify this, we have analyzed only the behavior of the transfer matrix M of Eq. (B4). This matrix describes the properties of the piezocomposite without taking into account the matching at $y=y_N$. Notice that the function $\tilde{u}_3(y_N)$ is calculated using Eq. (B6) which in turn comes from boundary conditions, Eqs. (33)–(35), at the free surface (the interface between the last layer and the vacuum). However, the calculation of M does not involve Eqs. (33)–(35). As a matter of fact, the block M_e of M (see Appendix B) is related with the transport properties of the system in a scattering problem.[17,24] So, in Fig. 4 we have also plotted $|(M_e)_{11}|^{-1}$ as a function of $\sin^2\theta$ (dashed line). $(M_e)_{11}$ is of course a dimensionless quantity. We see that this curve has the same structure as the continuous curve (solid line) except that the resonance around $\sin^2\theta=0.18$ is absent, a confirmation that this resonance is due to the surface states.

When the periodicity is broken [$F\neq 0$ in Eq. (17), or $\mathfrak{I} \neq 0$ in Eq. (28)], the structure of $|\tilde{u}_3(y_N)/A_{-1}|$ changes, as is shown in Fig. 5. A series of resonances is evident: the SLR, with a separation around the value $\Delta S = p c_{44}^{(-1)}(\frac{1}{4}) \times 10^{-7} = 0.2$ as predicted by Eq. (27). Indeed, there exist intervals of values for the parameters where the curves evolve from a band structure to a SLR structure. However, in this paper we do not show such an evolution. See, for example, Refs. 25, 26 for the case of SLR in the electronic spectrum. The curve for $|(M_e)_{11}|^{-1}$ is not shown in Fig. 5 because it is almost equal to the curve for $|\tilde{u}_3(y_N)/A_{-1}|$. In this case the presence of the surface states is not evident.

We have not observed SLR in all cases when $\mathfrak{I}\neq 0$. This occurs also in quantum, electromagnetic, and elastic SLR,[13,17,26,30] where there are several factors that affect the existence of SLR. As a matter fact, for the piezoelectric case there are more parameters than in the other cases, and the SLR are more unstable. It is also more difficult to find a set of parameters in order to have clear SLR as the ones shown in Fig. 5. Instead, the band structure is always easily found. Since $0 \leqslant \sin^2\theta \leqslant 1$, one has a very restrictive interval where the SLR could exist. In this sense, the numerical calculations will be very useful in order to observe SLR in the laboratory. In general, the effect of an arbitrary variation of the parameters on the SLR is complicated. In some cases the SLR are destroyed, in others they are modified and in others they survive without changes. For example, a simultaneous variation of the quantities F, p, and ω in such a way that the values of $\Delta S = p\,\mathfrak{I} c_{44}^{(-1)}$ and $p/\lambda = 2\pi p/k$ remain invariant, has no effect on the form of the curves. This is because ΔS gives the separation between resonances and λ/p gives the number of waves inside the period p. The quotient λ/p regulates the possibility that a resonance can be present (as in the Fabry-Perot interferometer).

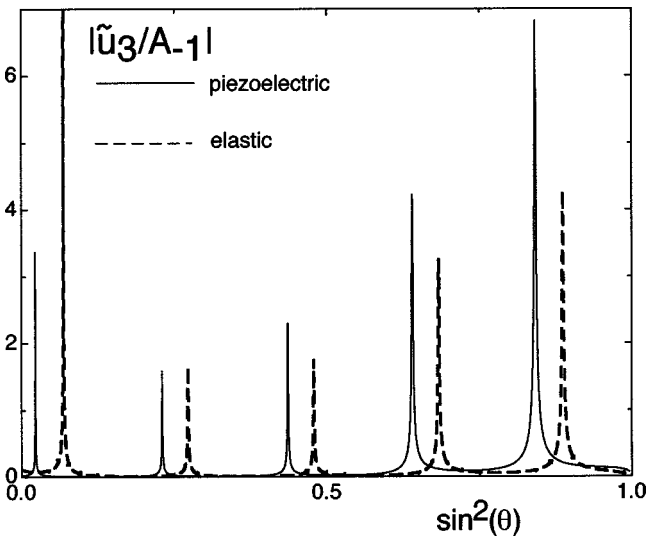

FIG. 5. The solid line is the plot of $|\tilde{u}_3(y_N)/A_{-1}|$ as a function of $\sin^2\theta$ for the piezocomposite of Fig. 1 for the case $F\neq 0$. The plot shows the SLR. The parameters ω and $e_{15}^{(-1)}$ are as in Fig. 4. The dashed line is also a plot of $|\tilde{u}_3(y_N)/A_{-1}|$ but for the pure elastic case. The curve also shows the SLR.

The effect of the piezoelectric moduli $e_{15}^{(n)}$ will be discussed in connection with Figs. 6 and 7. Since our formulation permits to describe the pure elastic case as well (it is sufficient to take the limit $e_{15}^{(n)} \to 0$ carefully in the corresponding equations) we have also analyzed this case which was first discussed by Mateos.[29] The dashed line in Fig. 5 shows the corresponding results for $|\tilde{u}_3(y_N)/A_{-1}|$. The presence of the SLR in the pure elastic case is evident as well.

In the Schrödinger equation case it has been established that each band gives rise to a Stark ladder[31] and in some intervals of energy more than one SL can coexist. In general the widths of the resonances belonging to a given SL are different to the ones associated with other SL's.[14,15] Furthermore, the relative position of the SL's changes as the parameters of the system change and some of the peaks disappear and others appear as discussed by Avron.[32,33] For the piezo-

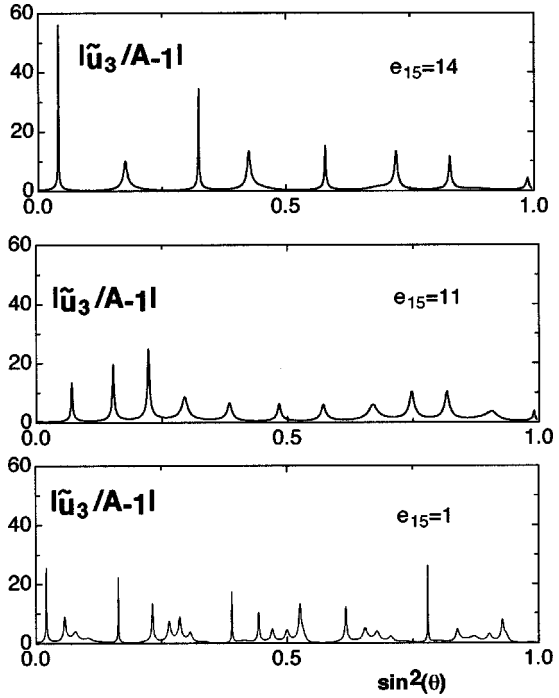

FIG. 6. The same as in Fig. 5 for three different values of $e_{15}^{(-1)}$. For clarity, we have omitted the superscript (-1) of e_{15} in the figures. The values of the parameters are those of Fig. 5 except $\omega = 2\times10^8$ s^{-1}, and $e_{15}^{(-1)}=1$, 11, 14 C/m^2.

electric case we have a similar behavior. For example, in Fig. 5 we have just only one SL. However, if we change the frequency to $\omega=2\times10^8$ s^{-1} we obtain the lower curve of Fig. 6, and when the piezoelectric modulus $e_{15}^{(-1)}$ is increased the upper curves of Fig. 6 are obtained. In the lower curve there are at least four SL's and three surface states, although they are not easily observed in this figure. However, more information can be obtained if the behavior of $|(M_e)_{11}|^{-1}$ is

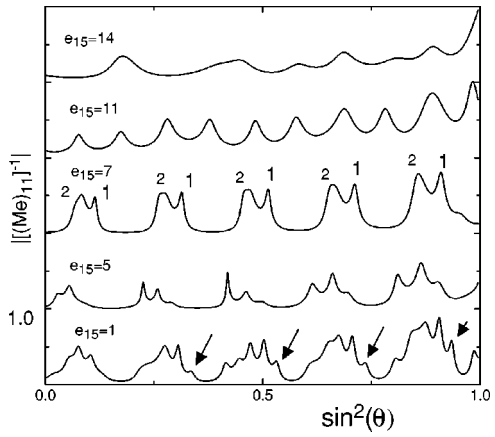

FIG. 7. The same as in Fig. 6 except that now the vertical axis indicates the values of $|(M_e)_{11}|^{-1}$ for five different values of $e_{15}^{(-1)}$: 1, 5, 7, 11, and 14 C/m^2. For clarity the curves have been vertically shifted except the curve $e_{15}^{(-1)}=1$. The range of vertical variation of the unshifted curves is [0,1]. In the third curve, we have indicated two Stark ladders labeled 1 and 2, and in the bottom curve the arrows indicate one of the Stark ladders.

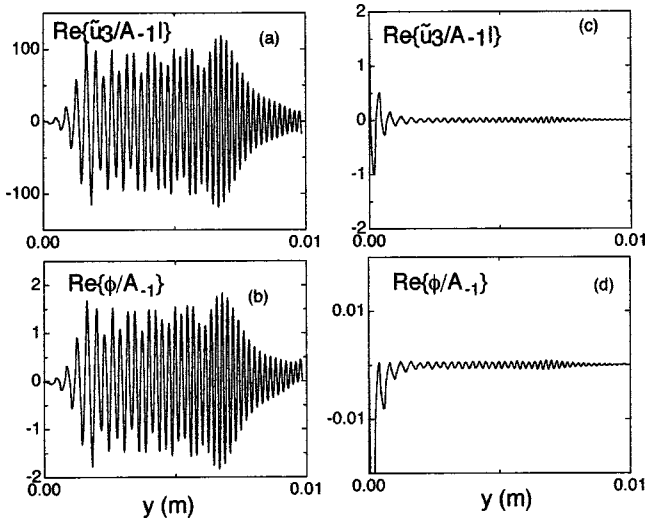

FIG. 8. (a,c) Plots of $\mathrm{Re}\{\tilde{u}_3(y)/A_{-1}\}$ as a function of y for angles of incidence θ such that $\sin^2\theta=0.023$ and $\sin^2\theta=0.09$, respectively. The first angle corresponds to the first resonance of Fig. 5(a). Note the different scales on the vertical axes. In (b) and (d) we have plots of $\mathrm{Re}\{\tilde{\phi}(y)/A_{-1}\}$ in units of N/C m as a function of y for the same values of θ, respectively.

analyzed, as in Fig. 7. In the lower curve we note clearly that the structure repeats itself with a period $\Delta S\approx0.2$ as predicted by Eq. (27) and it does not have the three surface states. One can identify four SL's in the curve (one of them labeled by the arrows) even though in some of the groupings we observe more than four peaks. When the piezoelectric modulus $e_{15}^{(-1)}$ is increased (see the upper curves) some of the peaks disappear and for $e_{15}^{(-1)}=7$ and 11 only two SL's are apparent (see also Fig. 6 where the surface states are not yet observed). For higher values of $e_{15}^{(-1)}$ the identification of the resonances is more difficult in both figures.

In Figs. 8(a) and 8(c) we have the values of the normalized displacement Re $\{\tilde{u}_3(y)/A_{-1}\}$ inside the piezocomposite, i.e., Re $\{\tilde{u}_3(y)/A_{-1}\}$ vs y. Figure 8(a) corresponds to an angle of incidence θ for which the system has a resonance [the resonance at $\sin^2\theta=0.023$ of Fig. 5(a)]. Figure 8(c) corresponds to a value of θ for which the system does not have resonance [$\sin^2\theta=0.09$ in Fig. 5(a)]. We observe that the mechanical displacement is appreciably different from zero inside the piezocomposite when the system has a resonance. Instead, for a nonresonant wave propagation the mechanical perturbation remains located near the left end of the system. This effect can be also observed in the potential. Figures 8(b) and 8(d) show plots of the normalized potential $\mathrm{Re}\{\tilde{\phi}/A_{-1}\}$ as a function of y. The values of $\sin^2\theta$ are again 0.023 and 0.09, respectively. As before, we observe that the potential is appreciably different from zero inside the systems only in a resonant configuration. In a nonresonant configuration the high values of the potential remain located near the left end of the system.

Some considerations can be made from the experimental point of view. The experimentalist can have a certain range of the parameters where the SLR and the bands should be

observed, although for the SLR case it is not easy to establish the conditions for the experiments accurately. The same situation can be found in other fields where SLR have been observed.[10,14,15] Some statistical studies on the stability of the SLR have been carried out in the quantum-mechanical case,[16] however, exact conditions under which the SLR can be measured are not yet stablished. In spite of this, some conditions for the existence of the SLR can be stated. For instance, since the SL appears as resonances in the plots $\tilde{u}_3$ vs $\sin^2\theta$ with $0 \leqslant \sin^2\theta \leqslant 1$, the distance between resonances,

$$\Delta S = \frac{pF\overline{c}_{44}^{(-1)}}{\omega^2 \rho^{(-1)}} = p\mathfrak{I} c_{44}^{(-1)}, \tag{36}$$

must be appreciably less than one in order to have some of them in the interval $[0,1]$ and to be able to identify a Stark ladder. Furthermore, since the presence of a resonance of this type is a phenomenon of interference—as in the case of a Fabri-Perot interferometer—we must have a period greater than a quarter wavelength, i.e.,

$$p \geqslant \frac{\lambda}{4} = \frac{\pi}{2k} = \frac{\pi v}{2\omega} = \frac{\pi}{2\omega}\sqrt{(1+\Omega\Gamma)}\sqrt{\frac{c_{44}^{(-1)}}{\rho^{(-1)}}}. \tag{37}$$

The size of the structure in the x direction should be appreciably greater than λ in order to avoid edge effects. As an example we have used the following set of parameters (see Table I), $p\omega \geqslant 2\pi \times 10^3$, $\Delta S = pc_{44}^{(-1)}(\frac{1}{4}) \times 10^{-7} = 0.2$, $\Omega = \frac{11}{4} \times 10^{-10}$, $\Gamma = (1/64.63) \times 10^{10}$ and we have obtained SLR. However, as was mentioned, the same structure of the SLR curves is obtained for simultaneous variation of the quantities $\mathfrak{I}$, p, and ω in such a way that ΔS and $p/\lambda = 2\pi p/k$ remain constant.

VI. CONCLUSIONS

In this work, we have calculated the displacement and electric potential amplifications at the free surface of a heterogeneous piezoelectric medium. We have obtained a band structure in the plots $\tilde{u}_3$ vs $\sin^2\theta$ according to the Bloch theorem for periodic composites under the incidence of electromechanical SH plane waves. However, for piezocomposites with a special monotonic variation of the material parameters we have observed the presence of SLR.

We have mentioned that the predictions of Wannier on the existence of SLR in the spectrum of electrons traveling through crystals in a dc electric field were correct, in spite of the fact that their reasoning had some weak arguments as pointed out by Zak.[7] For the piezoelectric case we have a similar situation; i.e., the extension of the reasoning of Wannier in order to predict SLR in the piezocomposites analyzed here also has weak points. Indeed, we now have an extra difficulty due to the fact that the complete solution involves the coupled functions u_3 and ϕ, where ϕ does not satisfy an equation such as the one used by Wannier. However, our numerical results show that the SLR indeed exist in piezocomposites, although they are more unstable as compared with the case of SLR studied in other types of systems.

ACKNOWLEDGMENTS

The work was supported by the CONACyT Grant Nos. 275020-A and J27710-T and the DGAPA-UNAM Grant Nos. IN114999, IN100197, and IN107599.

APPENDIX A: FUNDAMENTAL EQUATIONS OF THE PIEZOELECTRICITY

The constitutive relations for piezoelectric materials with $6mm$ crystal class, for each layer of the composite using the abbreviated vectorial notation, are given by[34,35]

$$\begin{bmatrix} T_1 \\ T_2 \\ T_3 \\ T_4 \\ T_5 \\ T_6 \\ D_1 \\ D_2 \\ D_3 \end{bmatrix} = \begin{bmatrix} c_{11} & c_{12} & c_{13} & 0 & 0 & 0 & 0 & 0 & -e_{31} \\ c_{12} & c_{11} & c_{13} & 0 & 0 & 0 & 0 & 0 & -e_{31} \\ c_{13} & c_{13} & c_{33} & 0 & 0 & 0 & 0 & 0 & -e_{33} \\ 0 & 0 & 0 & c_{44} & 0 & 0 & 0 & -e_{15} & 0 \\ 0 & 0 & 0 & 0 & c_{44} & 0 & -e_{15} & 0 & 0 \\ 0 & 0 & 0 & 0 & 0 & c_{66} & 0 & 0 & 0 \\ 0 & 0 & 0 & 0 & e_{15} & 0 & \epsilon_{11} & 0 & 0 \\ 0 & 0 & 0 & e_{15} & 0 & 0 & 0 & \epsilon_{11} & 0 \\ e_{31} & e_{31} & e_{33} & 0 & 0 & 0 & 0 & 0 & \epsilon_{33} \end{bmatrix} \times \begin{bmatrix} S_1 \\ S_2 \\ S_3 \\ S_4 \\ S_5 \\ S_6 \\ E_1 \\ E_2 \\ E_3 \end{bmatrix}. \tag{A1}$$

For simplicity, we omitted the superscript (n) for each layer in these basic equations. The z direction is the axis of six-order symmetry, $\mathbf{D} = (D_1, D_2, D_3)$ is the electric displacement. S_i $(i = 1, \ldots, 6)$ are the components of the strain tensor $\overleftrightarrow{S}$, which is defined in terms of the components of the displacement vector (u_1, u_2, u_3) as

$$\vec{\vec{S}} \equiv \begin{bmatrix} S_1 \\ S_2 \\ S_3 \\ S_4 \\ S_5 \\ S_6 \end{bmatrix} = \begin{bmatrix} \frac{\partial}{\partial x} & 0 & 0 \\ 0 & \frac{\partial}{\partial y} & 0 \\ 0 & 0 & \frac{\partial}{\partial z} \\ 0 & \frac{\partial}{\partial z} & \frac{\partial}{\partial y} \\ \frac{\partial}{\partial z} & 0 & \frac{\partial}{\partial x} \\ \frac{\partial}{\partial y} & \frac{\partial}{\partial x} & 0 \end{bmatrix} \begin{bmatrix} u_1 \\ u_2 \\ u_3 \end{bmatrix}. \tag{A2}$$

$\mathbf{E}=(E_1,E_2,E_3)$ is the electric field, which in the quasistatic approximation is related with the electrostatic potential ϕ by the formula

$$\mathbf{E}=-\nabla\phi. \tag{A3}$$

$\vec{\vec{T}}$ is the stress tensor that in matrix notation is written as

$$\vec{\vec{T}} \equiv \begin{bmatrix} T_1 & T_6 & T_5 \\ T_6 & T_2 & T_4 \\ T_5 & T_4 & T_3 \end{bmatrix}. \tag{A4}$$

We are using the reduced notations $T_1=T_{xx}$, $T_2=T_{yy}$, $T_3=T_{zz}$ for the diagonal components and $T_4=T_{yz}$, $T_5=T_{xz}$, and $T_6=T_{xy}$ for the off-diagonal components. The same notation is used for the strains S_i $(i=1,\ldots,6)$.

Substituting the above relations in the dynamic equation of elasticity and in the Gauss equation for electromagnetism:

$$T_{ij,j}=\rho\ddot{u}_i, \tag{A5}$$

$$D_{i,i}=0, \tag{A6}$$

we finally obtain the complete system of dynamic equations for a piezoelectric medium

$$c_{11}\frac{\partial^2 u_1}{\partial x^2}+c_{66}\frac{\partial^2 u_1}{\partial y^2}+c_{44}\frac{\partial^2 u_1}{\partial z^2}+(c_{66}+c_{12})\frac{\partial^2 u_2}{\partial x\partial y}+(c_{13}+c_{44})\frac{\partial^2 u_3}{\partial x\partial z}+(e_{31}+e_{15})\frac{\partial^2\phi}{\partial x\partial z}=\rho\ddot{u}_1, \tag{A7}$$

$$c_{66}\frac{\partial^2 u_2}{\partial x^2}+c_{11}\frac{\partial^2 u_2}{\partial y^2}+c_{44}\frac{\partial^2 u_2}{\partial z^2}+(c_{66}+c_{12})\frac{\partial^2 u_1}{\partial x\partial y}+(c_{13}+c_{44})\frac{\partial^2 u_3}{\partial y\partial z}+(e_{31}+e_{15})\frac{\partial^2\phi}{\partial y\partial z}=\rho\ddot{u}_2, \tag{A8}$$

$$c_{44}\left(\frac{\partial^2 u_3}{\partial x^2}+\frac{\partial^2 u_3}{\partial y^2}\right)+c_{33}\frac{\partial^2 u_3}{\partial z^2}+(c_{13}+c_{44})\left(\frac{\partial^2 u_1}{\partial x\partial z}+\frac{\partial^2 u_2}{\partial y\partial z}\right)+e_{15}\left(\frac{\partial^2\phi}{\partial x^2}+\frac{\partial^2\phi}{\partial y^2}\right)+e_{33}\frac{\partial^2\phi}{\partial z^2}=\rho\ddot{u}_3, \tag{A9}$$

$$e_{15}\left(\frac{\partial^2 u_1}{\partial x\partial z}+\frac{\partial^2 u_2}{\partial y\partial z}+\frac{\partial^2 u_3}{\partial x^2}+\frac{\partial^2 u_3}{\partial y^2}\right)+e_{31}\left(\frac{\partial^2 u_1}{\partial x\partial z}+\frac{\partial^2 u_2}{\partial y\partial z}\right)+e_{33}\frac{\partial^2 u_3}{\partial z^2}-\epsilon_{11}\left(\frac{\partial^2\phi}{\partial x^2}+\frac{\partial^2\phi}{\partial y^2}\right)-\epsilon_{33}\frac{\partial^2\phi}{\partial z^2}=0. \tag{A10}$$

APPENDIX B: TRANSFER MATRIX

Using conditions (29)–(32) we obtain the partial transfer matrix denoted by $M_{(n-1,n)}$, which relates the coefficients A_n, B_n, C_n, D_n associated to the solution at the n layer, as indicated in Eqs. (12) and (13), with the coefficients A_{n-1}, B_{n-1}, C_{n-1}, D_{n-1} associated to the solution at the $(n-1)$ layer by means of the expression

$$\begin{pmatrix} A_n \\ B_n \\ C_n \\ D_n \end{pmatrix} = M_{(n-1,n)} \begin{pmatrix} A_{n-1} \\ B_{n-1} \\ C_{n-1} \\ D_{n-1} \end{pmatrix}, \tag{B1}$$

with $0\leqslant n\leqslant N-1$. The transfer matrix $M_{(n-1,n)}$ has the following form:

$$M_{(n-1,n)} = -\frac{1}{2}\begin{pmatrix} -\alpha e^{iy_n\Delta} & -\beta e^{-iy_n\Sigma} & \delta e^{\Xi} & -\delta e^{-\Theta} \\ -\beta e^{iy_n\Sigma} & -\alpha e^{-iy_n\Delta} & -\delta e^{\Theta} & \delta e^{-\Xi} \\ \gamma e^{iy_n k_y^{n-1}} & \gamma e^{-iy_n k_y^{n-1}} & -\eta e^{k_x\Upsilon} & -\xi e^{-k_x\Upsilon} \\ \gamma e^{iy_n k_y^{n-1}} & \gamma e^{-iy_n k_y^{n-1}} & -\xi e^{k_x\Upsilon} & -\eta e^{-k_x\Upsilon} \end{pmatrix}, \tag{B2}$$

where

$$(k_y^n)^2 \equiv \frac{\omega^2\rho^{(n)}}{\overline{c_{44}^{(n)}}}-k_x^2=k_y^2(y) \quad \text{for} \quad y_n<y<y_{n+1},$$

$$\alpha=\left(1+\frac{k_y^{n-1}\overline{c_{44}^{(n-1)}}}{k_y^n\overline{c_{44}^{(n)}}}\right), \quad \beta=\left(1-\frac{k_y^{n-1}\overline{c_{44}^{(n-1)}}}{k_y^n\overline{c_{44}^{(n)}}}\right),$$

$$\gamma=\left(1-\frac{e_{15}^{(n-1)}\epsilon_{11}^{(n)}}{e_{15}^{(n)}\epsilon_{11}^{(n-1)}}\right), \quad \delta=i\frac{k_x(e_{15}^{(n-1)})^2}{k_y^n\overline{c_{44}^{(n)}}\epsilon_{11}^{(n-1)}}\left(1-\frac{e_{15}^{(n)}\epsilon_{11}^{(n-1)}}{e_{15}^{(n-1)}\epsilon_{11}^{(n)}}\right),$$

$$\eta=\left(\frac{e_{15}^{(n-1)}\epsilon_{11}^{(n)}}{e_{15}^{(n)}\epsilon_{11}^{(n-1)}}+\frac{e_{15}^{(n-1)}}{e_{15}^{(n)}}\right), \quad \xi=\left(\frac{e_{15}^{(n-1)}\epsilon_{11}^{(n)}}{e_{15}^{(n)}\epsilon_{11}^{(n-1)}}-\frac{e_{15}^{(n-1)}}{e_{15}^{(n)}}\right),$$

$$\Delta=(k_y^{n-1}-k_y^n),\quad \Sigma=(k_y^n+k_y^{n-1}),$$

$$\Xi=(k_x\Upsilon-iy_nk_y^n),\quad \Theta=(k_x\Upsilon+iy_nk_y^n),$$

$$\Upsilon=y_n-y_{n-1}.$$

The total transfer matrix M of order (4×4) defined as the product

$$M=M_{(N-2,N-1)}\cdot M_{(N-3,N-2)}\cdots M_{(n-1,n)}\cdots M_{(0,1)}\cdot M_{(-1,0)} \tag{B3}$$

relates the coefficients A_{-1}, B_{-1}, C_{-1}, D_{-1} of the left semi-infinite medium $(n=-1)$ with the coefficients A_{N-1}, B_{N-1}, C_{N-1}, D_{N-1} of the last layer $(n=N-1)$ by means of the expression

$$\begin{pmatrix}A_{N-1}\\B_{N-1}\\C_{N-1}\\D_{N-1}\end{pmatrix}=M\begin{pmatrix}A_{-1}\\B_{-1}\\C_{-1}\\D_{-1}\end{pmatrix}. \tag{B4}$$

According to our model and the considerations given in Eqs. (22)–(24), it can be shown that $\gamma=\delta=0$ in each layer and therefore the transfer matrix $M_{(n-1,n)}$ becomes a block diagonal matrix, i.e.,

$$M_{(n-1,n)}=\begin{pmatrix}M_{11_{(2\times2)}} & 0_{(2\times2)}\\ 0_{(2\times2)} & M_{22_{(2\times2)}}\end{pmatrix}$$
$$\text{for all}\quad n=0,1,\ldots,N-1. \tag{B5}$$

Consequently, M of Eq. (50) is also a diagonal matrix by blocks of order (2×2), where its first block different from zero will be denoted by M^e and the second one by M^s. The block $M_{11_{(2\times2)}}$ of each matrix $M_{(n-1,n)}$ has the same form as in the pure elastic case.[23,24,31] Furthermore, it can be shown that in our model the quotient $k_y^{n-1}\overline{c}_{44}^{(n-1)}/(k_y^n\overline{c}_{44}^{(n)})$, appearing in the quantities α and β, has exactly the same value as in the pure elastic case, i.e., $k_y^{n-1}\overline{c}_{44}^{(n-1)}/(k_y^n\overline{c}_{44}^{(n)})=\kappa_y^{n-1}c_{44}^{(n-1)}/\kappa_y^nc_{44}^{(n)}$, where κ_y^{n-1} is the value of k_y^{n-1} for the elastic case. However, $M_{11_{(2\times2)}}$ is still a function of the piezoelectric parameters since they are present in the expression for k_y^n which is contained in the factors $e^{iy_n\Delta}$, $e^{-iy_n\Sigma}$. Therefore, the product matrix M^e depends on the piezoelectric parameters as well. It was possible to observe this feature in the numerical result.

Since the matricial equation (B4) together the three equations (33)–(35) imply seven linear relations between the coefficients A_{-1}, B_{-1}, C_{-1}, D_{-1}, A_{N-1}, B_{N-1}, C_{N-1}, D_{N-1} we have eight conditions (including the normalization condition given by the value of A_{-1}) in order to determine the same number of unknown coefficients and the problem is solved, as we show below.

Using the boundary conditions (33)–(35) we obtain the following system of algebraic equations for determining the coefficients A_{N-1}, B_{N-1}, by means of which we obtain the displacement u_3 at the right end of the composite,

$$\begin{pmatrix}A_{N-1}\\B_{N-1}\end{pmatrix}=\left(\frac{C_{44}^{(-1)}k_y^{(-1)}}{C_{44}^{(N-1)}k_y^{(N-1)}}M^f+\frac{1}{\det}M^e\right)\times\left[\begin{pmatrix}1\\\Psi_o-1\end{pmatrix}-\frac{C_{44}^{(N-1)}}{C_{44}^{(-1)}}\begin{pmatrix}0\\\chi\end{pmatrix}\right], \tag{B6}$$

where

$$M^f=\begin{pmatrix}\left[M_{12}^e\left(\frac{h_{22}}{h_{11}}\right)+M_{22}^e-\frac{2}{h_{11}}\frac{C_{44}^{(-1)}}{C_{44}^{N-1}}e^{-k_xy_{-1}}\right]^{-1} & 0\\ -\left[M_{12}^e+M_{22}^e\left(\frac{h_{11}}{h_{22}}\right)-\frac{2}{h_{22}}\frac{C_{44}^{(-1)}}{C_{44}^{N-1}}e^{-k_xy_{-1}}\right]^{-1} & 0\end{pmatrix},$$

$$\chi=\left(\frac{1}{2}e^{-k_x\Upsilon'}(m_{22}^se^{-k_xy_{-1}}-m_{21}^se^{k_xy_{-1}})+\frac{1}{2}e^{k_x\Upsilon'}(m_{11}^se^{k_xy_{-1}}-m_{12}^se^{-k_xy_{-1}})\right)\Psi_N,$$

$$\Psi_0=\frac{\epsilon_{11}^{(-1)}}{e_{15}^{(-1)}}\phi_0,\quad \Psi_N=\frac{\epsilon_{11}^{(N-1)}}{e_{15}^{(N-1)}}\phi_N,$$

$$h_{11}=e^{-ik_y^{(N-1)}y_N}(r_2p_1e^{-k_x\Upsilon'}-r_1p_2e^{k_x\Upsilon'}),\quad h_{22}=\overline{h}_{11},$$

$$r_1=1+i\frac{k_y^{(N-1)}}{k_x}\left(1+\frac{1}{\delta\Omega}\right),\quad r_2=\overline{r}_1,$$

$$p_1=M_{22}^se^{-2k_xy_{-1}}-M_{21}^s,\quad p_2=M_{12}^se^{-2k_xy_{-1}}-M_{11}^s,$$

and

$$\det=1-\frac{1}{2}\frac{C_{44}^{(N-1)}}{C_{44}^{(-1)}}e^{k_xy_{-1}}(M_{12}^eh_{22}+M_{22}^eh_{11}),$$

$$\Upsilon'=y_N-y_{N-1}. \tag{B7}$$

The coefficients C_{N-1} and D_{N-1} can be calculated from the following expression:

$$\begin{pmatrix}C_{N-1}\\D_{N-1}\end{pmatrix}=-\begin{pmatrix}r_1e^{\Xi'} & r_2e^{-\Theta'}\\ r_2e^{\Theta'} & r_1e^{-\Xi'}\end{pmatrix}\begin{pmatrix}A_{N-1}\\B_{N-1}\end{pmatrix}+\frac{1}{2}\begin{pmatrix}e^{-k_x\Upsilon'}\\e^{k_x\Upsilon'}\end{pmatrix}\Psi_N, \tag{B8}$$

where

$$\Xi'=(iy_Nk_y^{N-1}-k_x\Upsilon'),\quad \Theta'=(k_x\Upsilon'+iy_Nk_y^{N-1}). \tag{B9}$$

The remaining coefficients A_{-1}, B_{-1}, C_{-1}, and D_{-1} can be obtained from Eq. (B4).

*Corresponding author. Email address: monsi@fisica.unam.mx

[1] E. Klein, J. Acoust. Soc. Am. **43**, 931 (1968).
[2] X. Geng and Q.M. Zhang, Appl. Phys. Lett. **67**, 3093 (1995).
[3] E.L. Adler, IEEE Trans. Ultrason. Ferroelectr. Freq. Control **37**, 485 (1990).
[4] B.A. Auld, Mater. Sci. Eng., A **122**, 65 (1989).
[5] A. Safaeinili, D.E. Chimenti, B.A. Auld, and S.K. Datta, Composites Eng. **5**, 1471 (1995).
[6] G.H. Wannier, Phys. Rev. **117**, 432 (1960); Rev. Mod. Phys. **34**, 645 (1962); *Elements of Solid State Theory* (Cambridge University Press, Cambridge, England, 1959), pp. 190–193.
[7] J. Zak, Phys. Rev. Lett. **20**, 1477 (1968); Phys. Rev. **181**, 1364 (1969).
[8] A. Rabinovitch, Phys. Lett. **33A**, 403 (1970).
[9] Curt A. Moyer, Phys. Rev. B **7**, 5025 (1973).
[10] A. Rabinovitch and J. Zak, Phys. Rev. B **4**, 2358 (1971).
[11] J.E. Avron, J. Zak, A. Grossmann, and L. Gunther, J. Math. Phys. **18**, 918 (1977).
[12] E.E. Mendez, F. Agulló-Rueda, and J.M. Hong, Phys. Rev. Lett. **60**, 2426 (1988).
[13] J.R. Banavar and D.D. Coon, Phys. Rev. B **17**, 3744 (1978).
[14] F. Bentosela, V. Grecchy, and F. Zironi, J. Phys. C **15**, 7119 (1982).
[15] F. Bentosela, V. Grecchy, and F. Zironi, Phys. Rev. Lett. **50**, 84 (1983).
[16] J.V. José, G. Monsivais, and J. Flores, Phys. Rev. B **31**, 6906 (1985).
[17] E. Cota, J.V. José, and G. Monsivais, Phys. Rev. B **35**, 8929 (1987).
[18] G. Monsivais, R. Rodríguez-Ramos, and L. Fernández-Álvarez, Ferroelectrics **268**, 233 (2002).
[19] C. Maerfeld and P. Tournois, Appl. Phys. Lett. **19**, 117 (1971).
[20] In this paper we discuss the existence of Stark ladders in piezoelectric systems from a theoretical point of view. The important issue for the validity of our formulation is that $\rho(y)\omega^2/\tilde{c}_{44}(y)$ has to satisfy a relation similar to that satisfied by $\mathcal{V}(x)$ given by Eq. (2). This condition can be fullfiled in many different cases and in this paper only some cases are considered. The fabrication details and engineering of multilayered piezocomposites are beyond the scope of this paper. However, there is abundant research in piezoelectric material engineering to achieve a wide range of values of piezoelectric parameters as the one we propose. See, for example, Refs. 21–25 and references therein.
[21] V.Z. Parton and B.A. Kudriavtsev, *Engineering Mechanics of Composite Structures* (CRC Press, 1993), p. 253.
[22] J.A. Otero, J. Bravo, and R.R. Ramos, Mech. Res. Commun. **24**, 75 (1997).
[23] J. Pastor, Mech. Res. Commun. **24**, 145 (1997).
[24] S. Torquato, *Random Heterogeneous Materials—Microstructure and Macroscopic Properties* (Springer-Verlag, New York, 2002).
[25] J. Bravo, J.A. Otero, R.R. Ramos, and A. Bourgeat, Int. J. Solids Struct. **35**, 527 (1998).
[26] G. Monsivais, M. del Castillo-Mussot, and F. Claro, Phys. Rev. Lett. **64**, 1433 (1990).
[27] C.M. Desterke, J.E. Sipe, and L.A. Wellerbrophy, Opt. Lett. **16**, 1141 (1991).
[28] M. del Castillo-Mussot and G. Monsivais, Solid State Commun. **92**, 925 (1994).
[29] J.L. Mateos and G. Monsivais, Physica A **207**, 445 (1994).
[30] G. Monsivais, F. García-Moliner, and V.R. Velasco, J. Phys.: Condens. Matter **7**, 5491 (1995).
[31] A. Rabinovitch, Phys. Lett. **59A**, 475 (1977).
[32] J. Avron, L. Gunther, and J. Zak, Solid State Commun. **16**, 189 (1975).
[33] J.E. Avron, Ann. Phys. **143**, 33 (1982).
[34] B.A. Auld, *Acoustic Fields and Waves in Solids* (Wiley-Interscience, New York, 1973).
[35] E. Dieulesaint and D. Royer, *Elastic Waves in Solids: Applications to Signal Processing* (Wiley, Chichester, 1980).